

# Surface and Interface Investigation of Indium-Tin-Oxide (ITO) Coated Nonwoven Fabrics

Qufu Wei\*, Huifeng Wang, Bingyao Deng and Yang Xu

Key Laboratory of Eco-textiles, Ministry of Education, Jiangnan University, Wuxi 214122, China

---

## Abstract

In this study, poly(ethylene terephthalate) (PET) nonwoven fabrics were used as substrates for creating functional nanostructures on the fiber surfaces. Magnetron sputtering was employed to deposit transparent and conductive indium-tin-oxide (ITO) nanofilms onto the nonwoven fabrics. The effects of the various deposition conditions on the surface and interfacial nanostructures were investigated by scanning electron microscopy (SEM), atomic force microscopy (AFM) and X-ray photoelectron spectroscopy (XPS). AFM observations revealed the effect of the deposition conditions on the morphology of the fibers. Surface chemical structures of the functional nonwoven fabrics were confirmed by XPS analysis. The interfacial structures were revealed by SEM examinations. The adhesion of the ITO coating to the fabric was investigated by the peel-off test. It was found that plasma pretreatment and heating during the sputter coating process obviously improved the adhesion of ITO coating to the PET fibers.

© Koninklijke Brill NV, Leiden, 2010

## Keywords

Adhesion, interface, indium-tin-oxide, nonwovens

## 1. Introduction

Textile materials in various forms have been expanding from conventional clothing and decoration markets into technical applications ranging from agriculture to space industries [1]. For a wide range of applications it is desirable to produce such textile materials with special surface structures and properties for particular applications. Textile materials with specific surface structures and properties are also of importance in many technical applications since many phenomena such as abrasion, friction, adhesion, adsorption, and biocompatibility are governed by the surface [2]. Surface modifications by various physical and chemical techniques are required to alter the surface properties of textile materials in order to meet different requirements [3–5].

---

\* To whom correspondence should be addressed. Tel.: 0086-510-85912007; Fax: 0086-510-85913200; e-mail: qfwei@jiangnan.edu.cn

Among the various physical techniques, physical vapor deposition (PVD) has become a promising method for the functionalization of textiles. PVD is basically a vaporization coating process involving an atom-by-atom or molecule-by-molecule transfer of material from the solid phase to the vapor phase and then deposition onto the surfaces of substrates [6]. Sputter coating is one of the most commonly used techniques in PVD, which has been widely used to deposit functional coatings onto glass, ceramic, polymer and textile substrates [7–9].

Transparent conducting oxides (TCOs) with special optoelectronic properties have attracted a great deal of attention in recent years due to their great potential in many industries. The most commonly used transparent conducting oxide is indium-tin-oxide (ITO) [10]. ITO films formed by different techniques have been increasingly used in a variety of applications, such as organic light emitting diodes (OLEDs), liquid crystal displays (LCDs), electromagnetic shielding and anti-ultraviolet devices.

In this work, ITO thin films were deposited on spunbonded nonwoven poly(ethylene terephthalate) (PET) fabrics by radiofrequency (RF) magnetron sputtering. The surface and interfacial structures were analyzed by scanning electron microscopy (SEM) and atomic force microscopy (AFM). The chemical structure of the deposited ITO on the fabrics was analyzed by XPS. The adhesion of the ITO coating to the textile substrate was investigated by the peel-off test.

Transparent conductive textiles offer great potential in flexible solar cells, electrodes, electromagnetic shielding and anti-ultraviolet applications.

## 2. Experimental

### 2.1. Substrate Preparation

The material used was spunbonded nonwoven PET fabric with a mass of 100 g/m<sup>2</sup>. The samples of the spunbonded nonwoven PET fabric were washed with acetone first and then rinsed twice with distilled water and finally dried in an oven at about 50°C prior to sputter deposition.

The pre-treatment of the PET fabric was performed using cold gas plasma to investigate the effect of the pretreatment on the adhesion of the ITO coating on the fabric. The plasma equipment used was a HD-1A (Changzhu, China) vertical laboratory plasma treatment machine. Oxygen was used as the treatment gas. The treatment conditions were set at a pressure of 10 Pa with a power of 50 W. The duration of the plasma treatment was 60 s.

### 2.2. ITO Deposition

The deposition of ITO on the PET fabric was performed using a magnetron sputter coating system JZCK-420B (Shengyan Juzhi, China). The nonwoven samples were placed in an ultra-high vacuum chamber with a base pressure of  $3 \times 10^{-4}$  Pa. The ITO target used was a ceramic target of 5 cm in diameter with a composition of 97 wt% In<sub>2</sub>O<sub>3</sub> and 3 wt% SnO<sub>2</sub>. Pure Ar (99.999%) was used as the sputtering gas.

**Table 1.**  
Description of samples used in this study

Sample	Sputtering conditions	
	Thickness (nm)	Temperature (°C)
1	50	Room
2	100	Room
3	200	Room
4*	100	Room
5	100	50
6	100	100
7	100	150
8	100	200

\* Sample was pre-treated by cold gas plasma.

The sputtering power used was set at 100 W with a gas flow of 20 sccm and pressure of 0.5 Pa. The thickness of the deposit was measured using a thickness monitor FTM-V (Taiyao, Shanghai) positioned in the sputtering chamber. The sample holder with a rotation speed of 100 rpm was introduced to improve the uniformity of ITO film deposited on PET fibers. The other conditions are detailed in Table 1.

### 2.3. Surface and Interface Observations

Atomic force microscopy (AFM) and scanning electron microscopy (SEM) were employed to examine the surfaces and interfaces of PET fibers after the deposition of functional ITO coatings. The AFM used was a CSPM 4000 (Benyuan, China). The scanning mode in the AFM was contact mode. All images were scanned at room temperature under ambient conditions. The SEM used was HITACHI S-4800 equipment.

### 2.4. XPS Analysis

XPS spectra were recorded on a photoelectron spectrometer (ESCA Lab MK II instrument, UK) using Mg  $K_{\alpha}$  radiation as the exciting source. All XPS spectra were calibrated with the C 1s peak at 284.6 eV.

### 2.5. Adhesion Testing

The adhesion of the sputtered ITO to the PET fabric surface was examined by the peel-off test. The test was performed on a Zwick Universal Testing Machine. The ITO coated fabric samples were cut into 7 cm  $\times$  2.5 cm for the peel-off test. The tape used for peeling was 3M-600 test adhesive tape. The tape was pressed onto the cut fabric samples with a load of 400 g for 12 h before the peel-off test. The initial peel distance between the tape and the fabric was 10 mm. The test speed was set at 200 mm/min. All tests were performed at  $20 \pm 2^{\circ}\text{C}$  and  $65 \pm 2\%$  RH

(relative humidity). Tests were carried out in triplicates and average values were reported.

### 3. Results and Discussion

#### 3.1. Surface Morphology

The surface morphology of the original PET fiber in the nonwoven fabric is presented in Fig. 1(a). The AFM image clearly reveals the smooth surface of the PET fiber in the nonwoven fabric with fibrils. The fibrils are formed along the fiber axis, as indicated in Fig. 1(a). The pre-treatment by cold plasma obviously alters the surface morphology of the PET fibers in the nonwoven fabric, as revealed in Fig. 1(b).

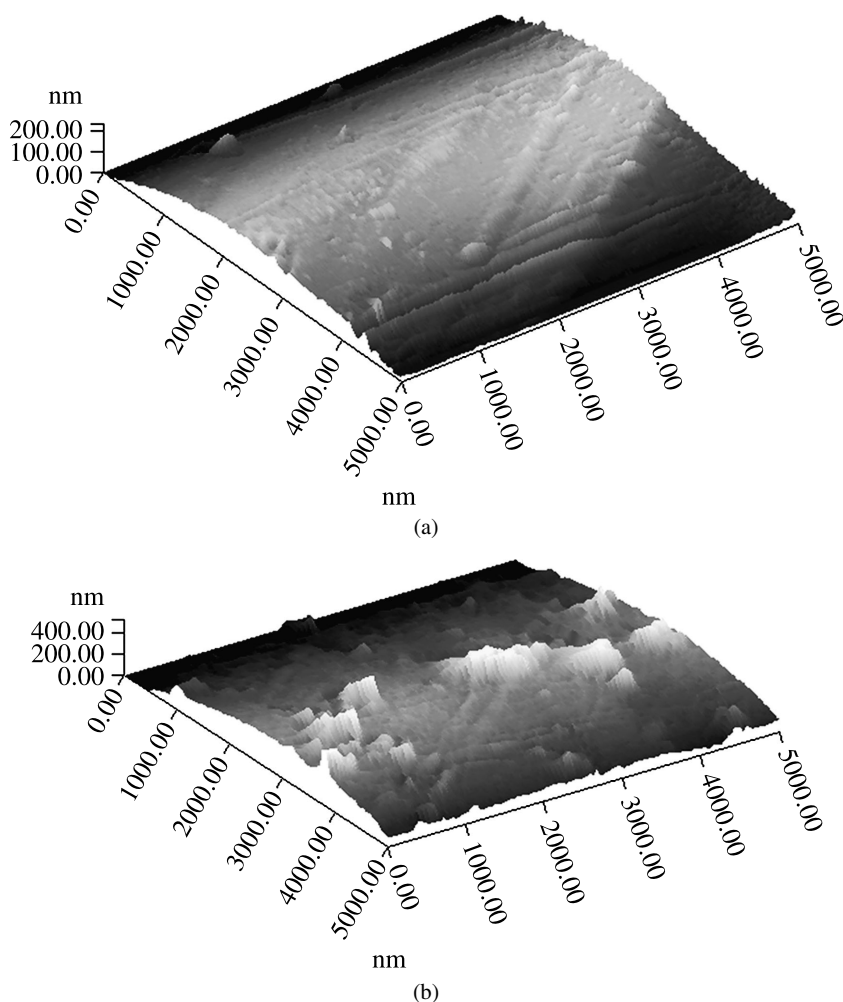
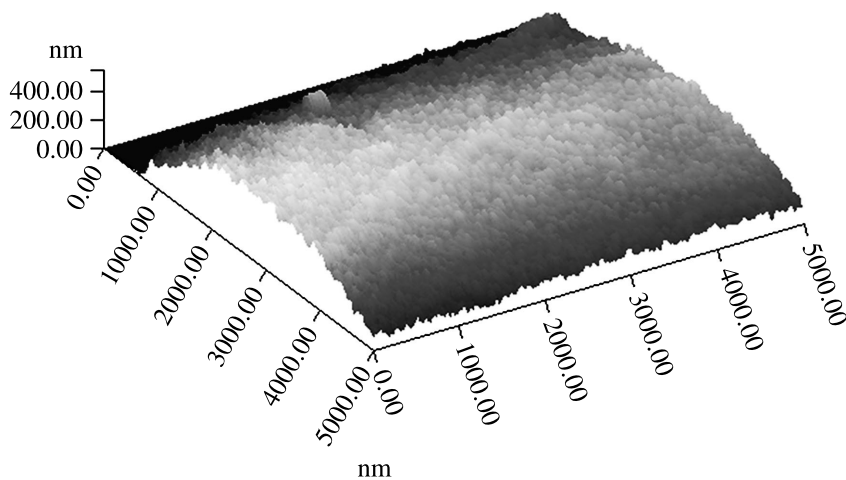


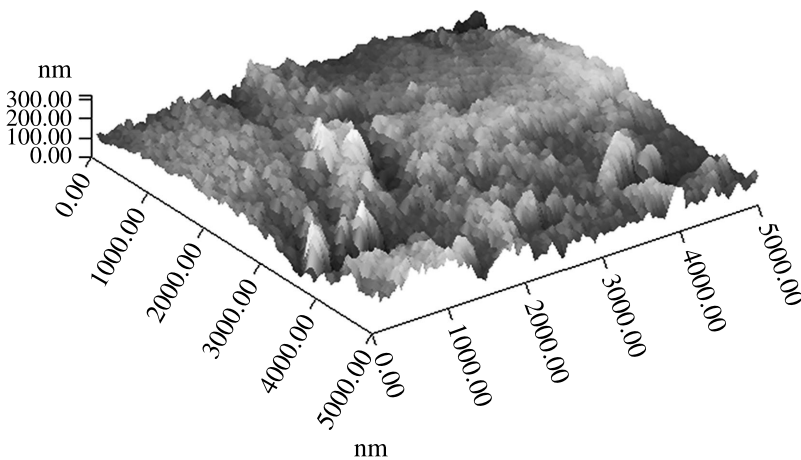
**Figure 1.** Surface morphology of PET fibers: (a) original; (b) plasma treated; (c) 50 nm ITO; (d) 100 nm ITO and (e) 200 nm ITO.

The image in Fig. 1(b) shows that the surface of the PET fiber is significantly roughened, which is attributed to the etching effect of the cold plasma treatment [11].

Figure 1(c) shows the surface of the PET fiber with 50 nm ITO coating. The high resolution AFM image clearly reveals the formation of nanoclusters on the PET fiber surface. The average size of the ITO clusters deposited on the PET fiber is about 12.5 nm as analyzed by the AFM software, and the coating thickness is 50 nm. The average size of the sputtered ITO clusters is increased to about 18.7 nm as the coating thickness reaches 100 nm. The image in Fig. 1(d) shows larger clusters formed on the PET fiber, compared to those shown in Fig. 1(c). The increase in the cluster size is attributed to the collision and growth of the sputtered particles when the deposition thickness is increased [12]. The size of the ITO clusters deposited on the PET fiber is further increased to about 24.9 nm when the coating thickness



(c)



(d)

**Figure 1.** (Continued.)

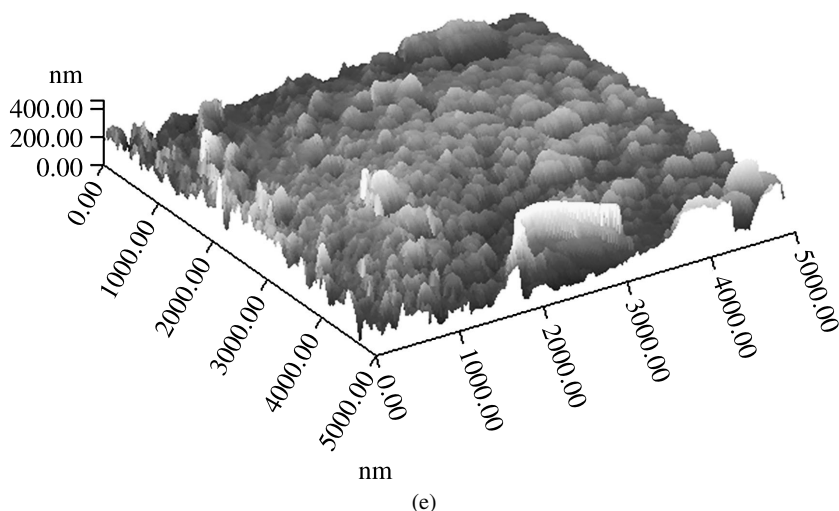


Figure 1. (Continued.)

reaches 200 nm. Figure 1(e) clearly shows the largest clusters deposited on the PET fiber surface.

The effect of temperature on the surface morphology of the ITO coated fibers is illustrated in Fig. 2. The growth of the ITO clusters formed on the PET fiber is observed as the coating temperature is increased to 50°C. The AFM image in Fig. 2(a) clearly shows the formation of larger ITO clusters on the fibers compared to those on the fiber with ITO sputtered at room temperature (Fig. 1(c)). The average size of the ITO clusters sputtered on the PET fiber at 50°C is about 21.3 nm. The increase in the cluster size is attributed to the collision of the sputtered ITO particles caused by higher energy at the higher temperature. The average size of the ITO clusters is further increased to about 24.6 nm as the temperature is increased to 100°C, as displayed in Fig. 2(b). The average size of the ITO clusters deposited on the PET fibers is further increased to about 28.9 nm, when the temperature reaches 200°C. The AFM image in Fig. 2(c) clearly reveals the roughest surface of the ITO coated PET fiber.

### 3.2. XPS Analysis

The chemical structure of the ITO deposited on the PET fiber is confirmed by XPS analysis, as presented in Fig. 3. The peaks at about 494.5, 486.0, 452.0 and 444.0 eV correspond to  $\text{Sn}3d_{3/2}$ ,  $\text{Sn}3d_{5/2}$ ,  $\text{In}3d_{3/2}$  and  $\text{In}3d_{5/2}$ , respectively. The peaks for  $\text{Sn}3d_{3/2}$  and  $\text{Sn}3d_{5/2}$  for the ITO coated fabric sample appear at around 494.5 eV and 486 eV respectively, as indicated in Fig. 3(a). The peaks at 486.3 and 494.6 eV analyzed by peak fitting are assigned to  $\text{Sn}^{4+}$  in  $\text{SnO}_2$ .

It is also found that the peaks for  $\text{In}3d_{3/2}$  and  $\text{In}3d_{5/2}$  of the ITO coated fabric sample appear at around 452 eV and 444 eV respectively, as illustrated in Fig. 3(b). The peaks at 445.5 and 453.3 eV analyzed by peak fitting are due to the presence of  $\text{In}^{3+}$  in  $\text{In}_2\text{O}_3$  [13].

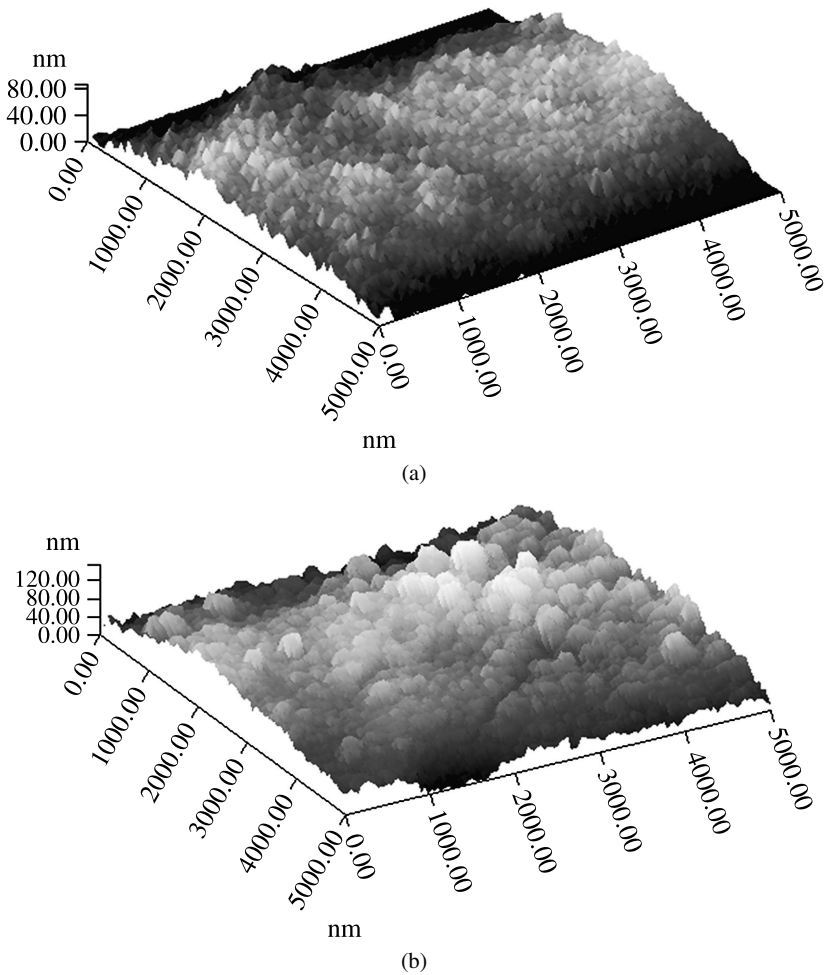


**Figure 2.** Surface morphology of PET fibers coated with 100 nm ITO at: (a) 50°C; (b) 100°C and (c) 200°C.

### 3.3. Adhesion Analysis

The results of the peel-off tests are listed in Table 2. Two groups of samples coated with ITO films were tested. For comparison purpose, the first group (samples 1–4) of samples was coated with ITO in different thicknesses (50 nm, 100 nm and 200 nm) and the second group (samples 5–8) of samples was prepared at different temperatures (50°C, 100°C, 150°C and 200°C).

Table 2 clearly reveals the effect of coating thickness and temperature on the peel-off force of the sputtered ITO coatings on the nonwoven PET fabric. It is observed that the peel-off force is increased from 3.3 N to 4.7 N as the ITO thickness is increased from 50 nm to 200 nm. The coating thickness contributes to the peel-off force due to the increased coverage of the thick coating as revealed in Fig. 1. It is

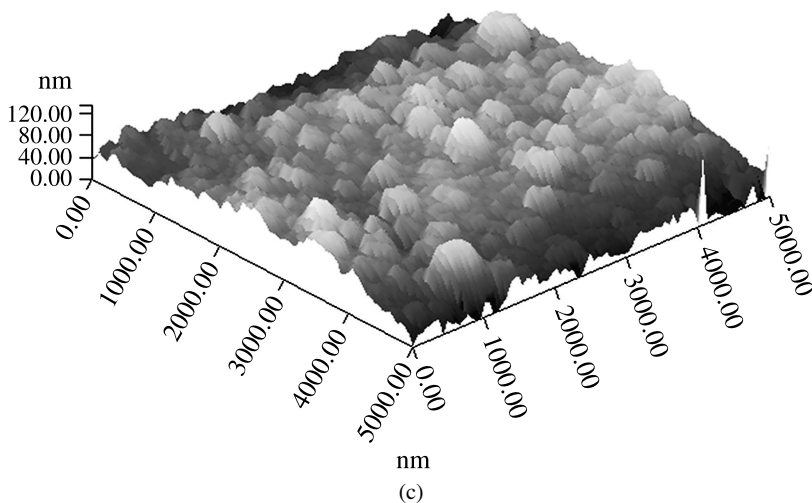


Figure 2. (Continued.)

also found that the standard deviation of the peel-off force decrease as the coating thickness is increased, as indicated in Table 2. This is also attributed to the coverage and compactness of the thick coating. It was believed that sputtered particles would strike the clusters previously deposited on the fibers and thus led to the compactness of the deposited grains [14]. The plasma treated sample has the highest peel-off force among all the samples tested. The plasma treatment roughens the surface of the PET fibers, facilitating through mechanical interlocking the adhesion of the deposited ITO clusters to the PET fiber surface. Plasma treatment not only roughened the surface as revealed in Fig. 1(b) but could also change the surface chemistry [11].

Table 2 shows that the adhesion of the ITO coating to the PET fibers is enhanced as the sputtering temperature is increased from room temperature to 150°C. The peel-off force is increased from about 4.3 N to 5.0 N when the sputtering temperature is increased from 50°C to 150°C. This could be attributed to the diffusion effect of the temperature. High temperature increases the energy of the sputtered ITO particles, leading to the penetration of the sputtered particles into the fiber surface. It is also observed from Table 2 that the standard deviation in peel-off force is reduced due to the improved adhesion of the ITO coating to the fabric. Table 2 indicates that the peel-off force is obviously decreased as the temperature is further increased to 200°C. The too high temperature may cause deformation of the fibers, damaging the ITO film deposited on the PET fiber surface. The largest standard deviation in the peel-off force indicates that the ITO film on the PET fiber is not stable and confirms the damage to the film deposited on the PET fibers at the high temperature.

### 3.4. Interfacial Analysis

The microstructures at the interface between the ITO coating and the PET fibers play an important role in the adhesion of coating layer to the substrate. The images

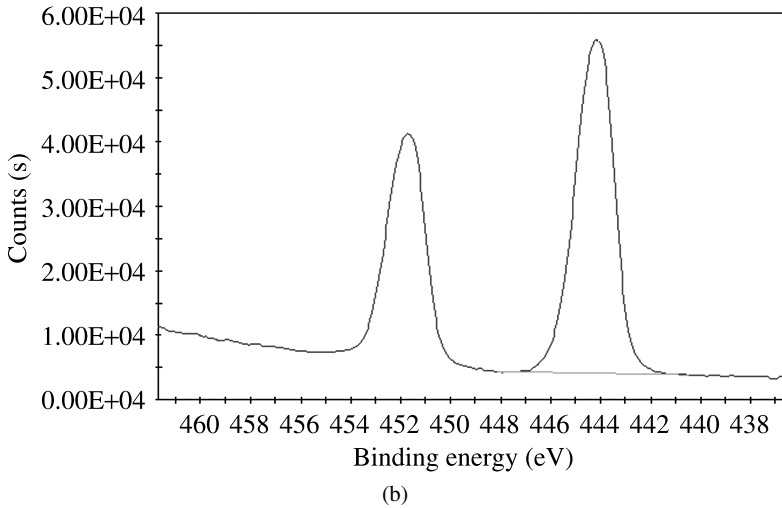
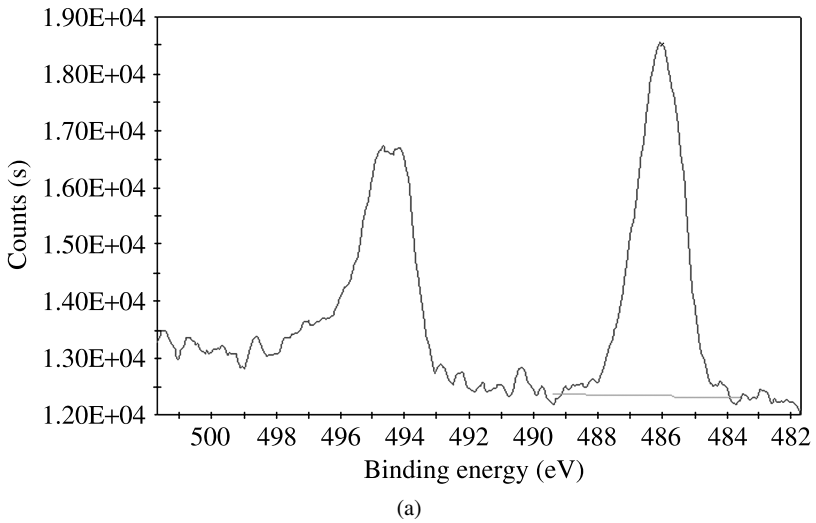


**Figure 3.** XPS spectra of ITO film deposited on PET fabric: (a) Sn3d spectrum and (b) In3d spectrum.

**Table 2.**

Results of peel-off force for different samples

Sample	Peel-off force (N)
1	$3.3 \pm 0.5$
2	$4.1 \pm 0.2$
3	$4.7 \pm 0.2$
4	$5.3 \pm 0.1$
5	$4.3 \pm 0.2$
6	$4.7 \pm 0.2$
7	$5.0 \pm 0.3$
8	$3.8 \pm 0.6$

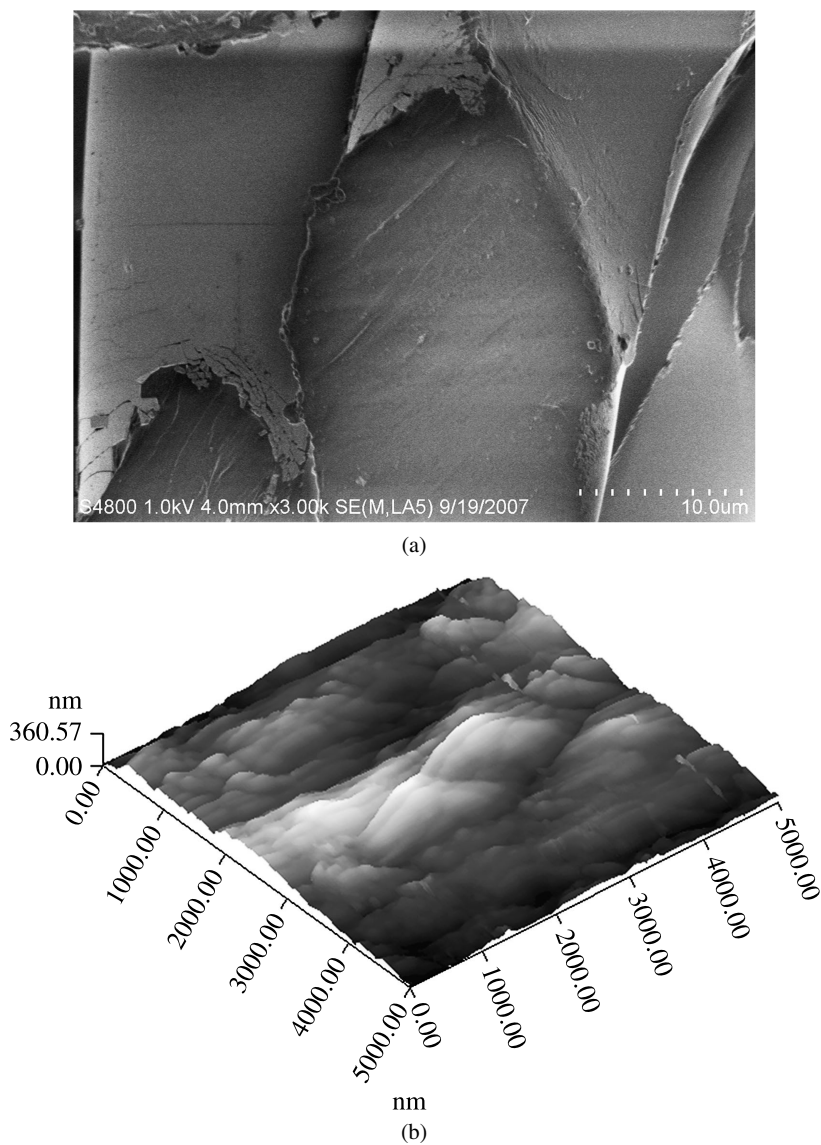
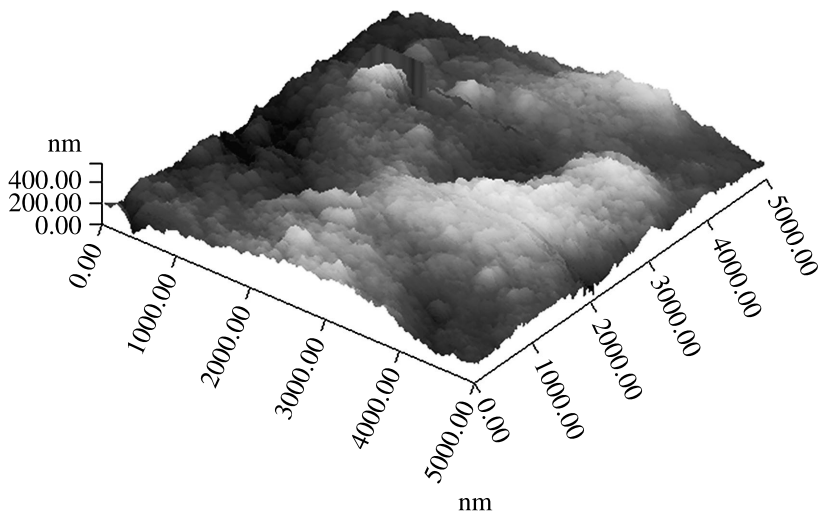
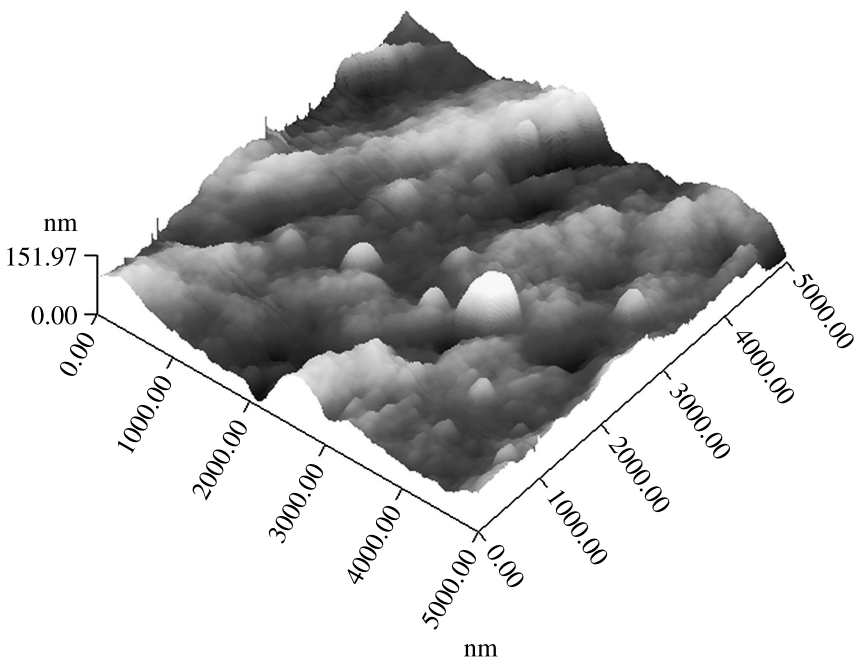


**Figure 4.** Interfaces of the PET fibers coated with 100 nm ITO before and after peel-off test: (a) SEM image of the cross section before peel-off test; (b) AFM image of the sample with ITO deposited at room temperature after peel-off test; (c) AFM image of the plasma treated sample with ITO deposited at room temperature after peel-off test and (d) AFM image of the sample with ITO deposited at 100°C after peel-off test.

in Fig. 4 illustrate the microstructures at the interface between of the ITO coating and PET fibers observed by SEM and AFM. The image in Fig. 4(a) clearly shows the interface formed on the ITO coated PET fibers. The ITO clusters are uniformly deposited on the PET fiber.



(c)



(d)

**Figure 4.** (Continued.)

The interfacial structures between the ITO clusters and the PET fibers were also observed by AFM. The image in Fig. 4(b) shows the interfacial structures of the ITO coated PET fibers after the peel-off test. The image shows separation of the ITO nanoclusters from the fiber surface after the peel-off test, indicating a poor adhesion of the sputtered nanoclusters to the PET fibers. Some residual ITO nanoclusters are

still visible, as indicated in Fig. 4(b). Figure 4(c) shows the surface of the ITO coated PET fibers after the peel-off test, in which the PET fibers were subjected to plasma pre-treatment. It is observed that the surface is much rougher compared to that of the untreated fibers in Fig. 4(b). The residual ITO clusters still cover the fiber surface after the peel-off test, revealing an improved adhesion of the ITO coating to the PET fibers. The effect of the temperature on the adhesion of the sputtered ITO coating on the PET fibers can also be observed in AFM. The image in Fig. 4(d) clearly shows that the sputtered ITO clusters appear to be embedded in the PET fiber matrix after the peel-off test, indicating an enhanced adhesion of the ITO coating to the PET fibers.

#### 4. Conclusion

The adhesion of the sputtered ITO films to the nonwoven PET fabric was investigated in this study. The surfaces and interfaces of the ITO coated PET fibers were examined by AFM and SEM. AFM and SEM images revealed the changes in surface and interface structures caused by different sputtering conditions. It was found that plasma pre-treatment roughened the PET fibers, leading to a better adhesion of the ITO coating to the PET fibers. The effect of the sputtering temperature was also analyzed. The increase in temperature to certain extent contributed to improvement in the adhesion of the ITO coating to the PET fibers, but too high temperature might damage the deposited coating.

#### Acknowledgements

The work was financially supported by the Program for New Century Excellent Talents in University (No. NCET-06-0485) and the Natural Science Foundation of Jiangsu Province (BK2008106).

#### References

1. D. Rigby and R. Jeffery, *International Textile Bulletin: Nonwovens, Industrial Textiles* **47** (3), 19–22 (2001).
2. M. R. Buchmeiser, *Monatshefte Chemie* **137**, 825–833 (2006).
3. Y. Dietzel, W. Przyborowski, G. Nocke, P. Offermann, F. Hollstein and J. Meinhardt, *Surface Coatings Technol.* **135**, 75–81 (2000).
4. H. J. Qi, D. Wang, Z. L. Ma, S. Q. Sun, Q. Y. Sui, W. P. Zhang and J. J. Lu, *J. Appl. Polym. Sci.* **85**, 1843–1850 (2002).
5. A. Bozzi, T. Yuranova, I. Guasaquillo, D. Laub and J. Kiwi, *J. Photochem. Photobiol. A* **174**, 156–164 (2005).
6. S. Cho, E. Kim, C. Kim, J. Noh, H. Choi, D. Park, T. Kwon, D. Yoo, I. Kim, S. O. Kim and D. Chung, *J. Korean Phys. Soc.* **45**, 623–626 (2004).
7. M. Y. Li, N. Chokshi, R. L. DeLeon, G. Tompa and W. A. Anderson, *Thin Solid Films* **515**, 7357–7363 (2007).

8. J. O. Carneiro, V. Teixeira, A. Portinha, A. Magalhães, P. Coutinho, C. J. Tavares and R. Newton, *Mater. Sci. Eng. B* **138**, 144–150 (2007).
9. Q. F. Wei, Q. Li, D. Y. Hou, Z. T. Yang and W. D. Gao, *Surface Coatings Technol.* **201**, 1821–1826 (2006).
10. S. K. Park, J. I. Han, W. K. Kim and M. G. Kwak, *Thin Solid Films* **397**, 49–55 (2001).
11. Q. F. Wei, Y. Liu, D. Y. Hou and F. L. Huang, *J. Mater. Proc. Technol.* **194**, 89–92 (2007).
12. Q. F. Wei, X. L. Xiao, D. Y. Hou, H. Ye and F. L. Huang, *Surface Coatings Technol.* **202**, 2535–2539 (2008).
13. A. De, P. K. Biswas and J. Manara, *Mater. Character.* **58**, 629–636 (2007).
14. O. Kluth, G. Schöpe, J. Hüpkes, C. Agashe, J. Müller and B. Rech, *Thin Solid Films* **442**, 80–85 (2003).